JOURNAL OF OPTOELECTRONICS AND ADVANCED MATERIALS, Vol. 10, No. 9, September 2008, p. 2482 - 2486

Corrosion environment detection using an evanescent light absorption technique

V. FOGEL, N. MIRCHIN, S. POPESCU, I. LAPSKER, A. PELED*
Holon Institute of Technology, EE Department, Photonics Laboratory
52 Golomb Str. Holon, Israel- 58102

Using the technique of capturing the evanescent light leaking image, we measured the influence of a corrosive environment on nanometric profiles of sputtered ultra-thin a-Au nano-structures of thicknesses in the range 20-90 nm. The films were deposited by sputtering directly on glass substrates serving also as light waveguides. Good agreement was achieved comparing the results of thickness and profiles evaluation for the ultra-thin a-Au nano-structures obtained from mechanical probe profile evaluation vs. the Differential Evanescent Light Intensity technique (DELI) estimations.

(Received August 10, 2008; accepted August 28, 2008)

Keywords: Nanometer layers, Evanescent field, Corrosion detection

1. Introduction

In this work we have investigated by a new optical microscopy technique named Differential Evanescent Light Intensity (DELI) easier to use then AFM or SEM the nanostructure morphology of amorphous Au (a-Au) sputtered thin films of thicknesses in the range of 20-90 nm.

A typical application of the DELI technique [1,2] is also as a corrosion detector by using materials of nanometer thickness and exposing them to corrosion influence.

Various nanometer waveguide based sensors and in particular Au based corrosion sensors have been published in the literature [3-7], thus we decided to test the combination of DELI with nanometer a-Au nanofilms.

The morphological investigation shows that the structures are amorphous spheroids observed on the glass substrates with diameters typically in the range of 100-300 nm as obtained by both DELI and SEM nanoprofiles microscopies.

The nano-structures investigated at high magnification by DELI in this work describe the morphology of the deposited a-Au nanofilms and after exposure to corrosive environment.

2. Deposition experimental procedure

The depositing procedures were as follows: We used a sputtering system run at about 1 mTorr and the deposited thickness d, defined according to a calibrated procedure bythe equation:

$$d = K \cdot I \cdot V \cdot t \qquad (1)$$

Where K is the Au calibration material constant, I is the plasma current, V is the voltage applied and t the time for deposition.

A square aperture of 10x10 mm was positioned above the glass substrate to obtain 7 square areas with various thicknesses in the range 10-100 nm. The glass substrates used were of borosilicate clear glass microscope slide type with dimensions of 75x25x1 mm. The experimental constant K was 0.17×10^{-10} when *I* was measured in mA, V in kV, t in seconds and d in nanometers. The source material was an Au plate of 99% purity and the films deposited were amorphous.

3. Nanometer films profile evaluation by DELI

The profiles of thin films of the a-Au squares were observed directly on the glass substrates by DELI [1].

Our technique of Differential Evanescent Light Imaging (DELI) used in this investigation is a version of the far field technique and has been developed to achieve a high resolution for nanometer features though only in the z-direction, $i \cdot e$, into the depth direction of the surface samples. The technique uses basically the phenomenon of Total Internal Reflection (TIR) [2] where evanescent waves arise.

This technique has the advantage that the far field image does not include direct transmitted or reflected light. In fact we rely on the evanescent light “extraction power" of the nanoparticles and nanolayers on the substrate which serves as optical waveguide also. We obtain usually an image in the far field since we are interested in large areas structural investigation but proximity imaging is also possible. The well known TIR phenomenon occurs when light passes from an optically denser medium n_1 which is the waveguide, into a less dense medium n_2. The transmitted electrical field is

described after a regular refraction incidence at the interface by:

$$E_t(x,t) = E_0 \cdot e^{-j\cdot\omega\cdot\left(t-\frac{n_1}{c}\cdot(x\cdot\sin\theta_i)\right)} \cdot e^{-\frac{n_2}{c}\cdot\omega\cdot z\cdot\sqrt{\left(\frac{n_1}{n_2}\cdot\sin\theta_i\right)^2-1}} \tag{2}$$

Where E_0 is the incident electrical field amplitude within the waveguide propagating in the x direction and in terms of the light intensity we have the following evanescent form in the depth z, direction:

$$I_{ew}(z) \sim I_0 \cdot e^{\frac{2\cdot z}{d}} \tag{3}$$

Where the evanescent characteristic penetration depth is defined by:

$$d = \frac{\lambda_{vac}}{2\cdot\pi\cdot\sqrt{\left(n_2^2\cdot\sin^2\theta_i - n_1^2\right)}} \quad (nm) \tag{4}$$

λ_{vac} is the vacuum wavelength of the light beam used in the waveguide

To observe the morphology we captured 2D images at several zooming powers of a microscope equipped with a CCD camera, down to the range of well resolved x-y areas as shown in Fig.1. As can be observed, the morphology at this resolving power gives for the sample shown, a typical surface structure of isolated spherical particles and interconnected spheroids. For the thicker samples we observed similar forms but with a higher connectivity and merging between the spheroids. It can also be seen that they are more bulky than the thinner samples.

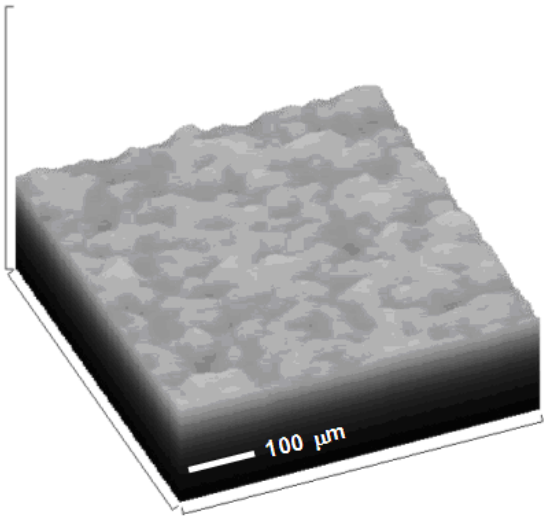

Fig.1: DELI 3D zoomed images of an a-Au sampled area of **500** × **500** *μm: with thicknesses of about 10 (nm). Bar size is 100 μm. Microscope magnification used was x 40.*

In Fig. 2 we show the 3D perspective profiles of 7 samples with thicknesses in the range 10-90 (nm).

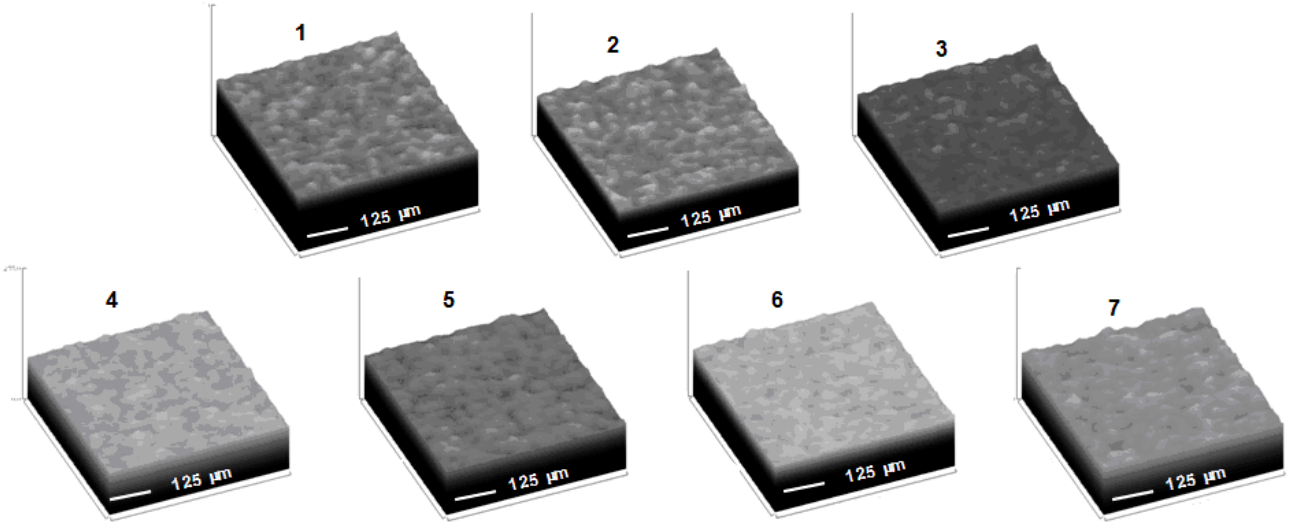

Fig.2. DELI 3D perspective zoomed images of 7 a-Au sampled areas with thicknesses in the range 10-90 nm. Bar size is 125 μm. Sampled zones areas are of size ~ 500x500 μm^2. Microscope magnification used was x 40.

To evaluate the relative and absolute surface nanoprofile thicknesses of the various samples in the z-direction we evaluated the mean Integrated Optical Density (IOD) in the deposited zones as shown in Fig.3.

The Normalized Integrated Optical Density (IOD) is defined as:

$$IOD = \frac{\iint_S D(x,y)\cdot ds}{D_{\max}\cdot S} = \frac{\int_0^\infty D\cdot H(D)dD}{I_0} \tag{5}$$

Where D(x, y) is the gray level value of each pixel (0-255) and S is the area of the sampled image. H (D) is the image histogram i.e., the number of pixels per gray level and I_0 is the mean surface integrated maximum Image Optical Density (IOD) obtained from the sampled image light intensity.

In the insets above the IOD curves the 2D captured 7 images of the samples shown in Fig.2 are given. We observe that the thickness increases from samples As1 to As7 corresponding to the calibrated thickness measurements during the deposition, the darker areas having less thickness.

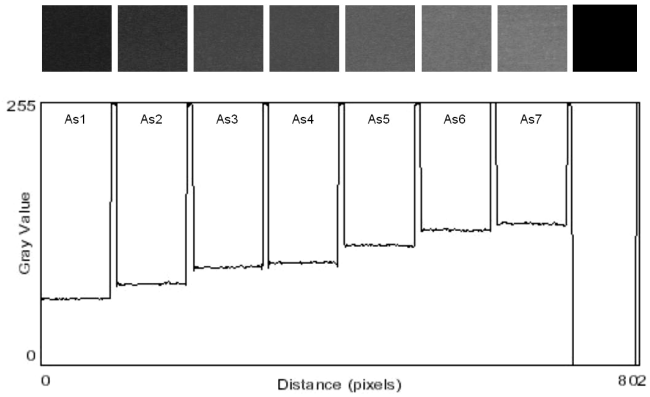

Fig. 3. DELI 2D images of 7 a-Au sampled areas profiles from Fig.2: with thicknesses in the range 10-90 nm. In the insets above the DELI profile plots we show the sampled areas as captured by the camera at x6.5 magnification of the microscope. Sampled zones areas are of size ~ 850x850 μm. Microscope magnification used was x 6.5. Last black square is for calibration purposes.

To calibrate the IOD thicknesses to absolute values we used sample As5 which was measured by a surface profilometer Surtronic 3, giving an average value of 70 nm. In previous papers [1,2] we have developed a phenomenological equation giving for normalized IOD values the following expression and approximation:

$$\frac{IOD_1}{IOD_2} = \frac{(1-e^{-\delta h_1})}{(1-e^{-\delta h_2})} \approx \frac{h_1}{h_2} \qquad (6)$$

Where h_k are the absolute film thickness values pertaining to the normalized IOD (h_k) values, $\delta^{-1} = d/2$ and k is the index specifying the sample As1-As7. We showed that this procedure is an accepted approximation for dielectric materials of nanometric thicknesses up to about 100 (nm). This equation and approximation was used here also to obtain the thickness values for all the other samples. In Fig.4 the DELI evaluation thickness from eqn(6) and as calculated thickness from eqn. (1) are shown vs. deposition time.

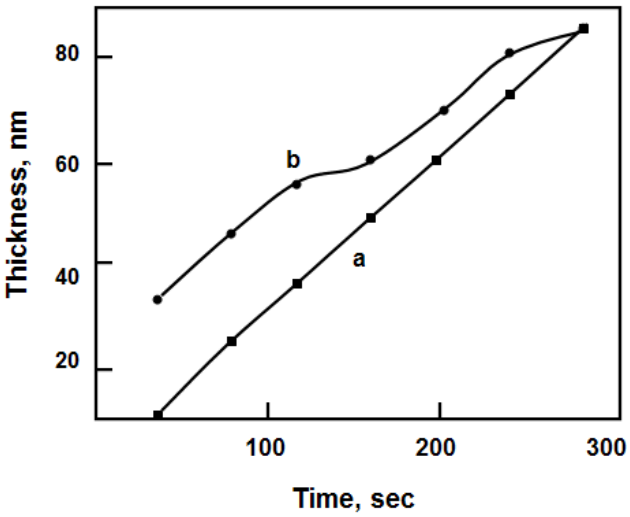

Fig .4. Plot of the thicknesses of 7 samples: curve (a) as calculated from eqn. (1) for the various samples as a function of deposition time and curve (b) from DELI calibrated by a surface profilometer Surtronic 3.

It is seen from Fig.4 that the thicknesses diverge at the lower end values but this is expected since we calibrated the DELI only at the high end thickness where the material is more compact.

4. Corrosive influence testing on the a-Au films

To test the sensitivity of the DELI technique to evaluate the corrosive influence on the a-Au films we exposed the samples to an etching solution of 70% HNO_3 for 4 seconds, then flushed them with pure water and dried air. Then we performed another DELI evaluation experiment of the nanometer samples and the calibrated thickness results are given in Fig. 5 for the samples before and after etching.

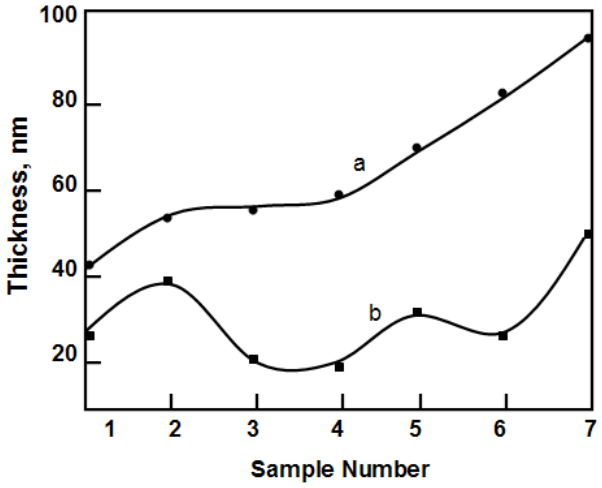

Fig. 5. Plot of the DELI thicknesses of the 7 samples: (a) before and (b) after etching in the corrosive solution.

Typically we observed for all samples a non uniform etching mechanism where some spikes of the a-Au are left on the surface and a lower level of amorphous valleys are created by the etching process. A typical morphological DELI 2D and 3D perspective of the As7 etched sample is shown in Fig. 6.

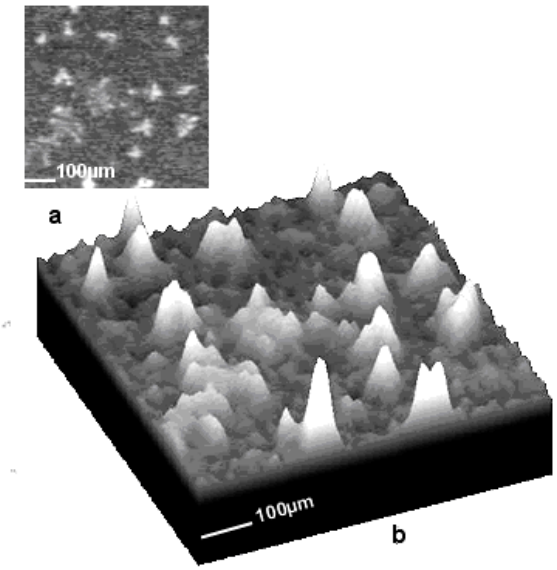

Fig.6. DELI 2D and 3D thicknesses profile of sample As7 after etching in the corrosive solution. The bars in both figures a and b are 100 µm. Magnification of microscope was × 6.5.

5. Discussion

This investigation showed that DELI can be a very easy and convenient method for observing qualitatively profiles of nanometer thickness a-Au nanolayers. If absolute measurements are required one has to use a calibration method for only one or a few samples by other absolute thickness measuring method like mechanical profilometer or SEM or spectroscopy. Then the DELI approximation given in eqn.(6) can be used to evaluate the absolute values of the profiles. In our case we observed from Fig. (4) that there is a divergence between the DELI absolute thickness for the lower end towards 10 nm thickness. This is expected taking into account that the amorphous Au films were not completely covered, i.e., the surface was an inhomogenous aggregation of spheroids, see Fig. (1) and the DELI technique cannot resolve spatially the tiny local features but rather give an integrated value of the far field light intensity emanating from the waveguide.

As for the etching process we observed that the DELI technique was sensitive enough to show the change in both average thickness of the films profiles and also to show the irregularity involved in the etching process, see Figs. (5) and (6).

6. Conclusions

The motivation for investigating the DELI method with a-Au nanometer-thin films was to assess the technique in terms of suitability and ease of use for morphological evaluation of nanometer thickness profiles. DELI is indeed a very sensitive differential-evanescent light diagnostic technique. We have realized that it is possible to calculate the thin films thickness for various a-Au-layers in the range of 10-90 nm. It was found also sensitive enough to quantify etching processes of nanolayers, thus suitable for corrosion environment sensors.The foremost specific advantages of the technique used is its simplicity and non-destructive features as compared to other more expensive nanosize evaluation methods such as SEM and AFM.

References

[1] G. Socol, E. Axente, M. Oane, L. Voicu, A. Petris, V. Vlad, I.N. Mihailescu, N. Mirchin, R. Margolin, D. Naot, A. Peled, Applied Surface Science **253**, 6535 (2007).

[2] G. Socol, E. Axente, M. Oane, L. Voicu, A. Dinescu, A. Petris, V. Vlad, I.N. Mihailescu, N. Mirchin, R. Margolin, D. Naot, A. Peled J. of Materials Science: Materials in Electronics, **18,** 207(2007).

[3] Abdelaziz Himour, Sihem Abderrahmane, Nasser Eddine Beliardouh, Moussa Zahzouh and Mokhtar

Ghers , Japanese Journal of Applied Physics **44**(9A), 6709 (2005).
[4] Mohammed Zourob, Stephan Mohr, Bernard J. Treves Brown, Peter R. Fielden, Martin McDonnell, Nicholas J. Goddard, Sensors and Actuators B **90,** 296 (2003).
[5] O. Galip Saracoglu, Sedat Ozsoy, Opt. Eng. **41**(3), 598 (2002).
[6] G.P. Wiederrecht, Eur. Phys. J. Appl. Phys. **28**, 3(2004).
[7] Kyoko Fujita, Keisuke Taniguchi, Hiroyuki Ohno , Talanta **65,** 1066 (2005).

*Corresponding author: peledddd@gmail.com